The Plant Cell, Vol. 7, 2091–2100, December 1995

ATP-Dependent Regulation of an Anion Channel at the Plasma Membrane of Protoplasts from Epidermal Cells of Arabidopsis Hypocotyls

Sébastien Thomine,[1] Sabine Zimmermann,[2] Jean Guern, and Hélène Barbier-Brygoo

Institut des Sciences Végétales, Centre National de la Recherche Scientifique, Bât 22, Avenue de la Terrasse, F-91198 Gif-sur-Yvette Cedex, France

Although Arabidopsis is the object of many genetic and molecular biology investigations, relatively few studies deal with regulation of its transmembrane ion exchanges. To clarify the role of ion transport in plant development, organ- and tissue-specific ion channels must be studied. We identified a voltage-dependent anion channel in epidermal cells of Arabidopsis hypocotyls, thus providing a new example of the occurrence of voltage-dependent anion channels in a specific plant cell type distinct from the stomatal guard cell. The Arabidopsis hypocotyl anion channel is able to function under two modes characterized by different voltage dependences and different kinetic behaviors. This switch between a fast and a slow mode is controlled by ATP. In the presence of intracellular ATP (fast mode), the channels are closed at resting potentials, and whole-cell currents activate upon depolarization. After activation, the anion current deactivates rapidly and more and more completely at potentials negative to the peak. In the absence of ATP, the current switches from this fast mode to a mode characterized by a slow and incomplete deactivation at resting potentials. In addition, the whole-cell currents can be correlated with the activity of single channels. In the outside-out configuration, the presence of ATP modulates the mean lifetimes of the open and closed states of the channel at hyperpolarized potentials, thus controlling its open probability. The fact that ATP-dependent voltage regulation was observed in both whole-cell and outside-out configurations suggests that a single type of anion channel can switch between two modes with distinct functional properties.

INTRODUCTION

Recent findings suggest important roles for anion channels in plant cells. In stomatal guard cells, anion channels, together with outward rectifying potassium channels, provide the pathways for ion efflux, leading to a decrease in cell turgor and thus to stomatal closure, whereas inward potassium channels allow the accumulation of potassium, leading to stomatal opening (Schroeder and Hedrich, 1989). The role of guard cell anion channels during stomatal closure has been demonstrated using pharmacological tools (Schroeder et al., 1993). Their regulation by external signals such as auxin and malate (Marten et al., 1991; Hedrich and Marten, 1993) points to them as mediators of stomatal responses to P_{CO_2} variations and auxin (Marten et al., 1991; Hedrich et al., 1994). They are also modulated by such intracellular signals as free calcium variations and nucleotides (Schroeder and Hagiwara, 1989; Hedrich et al., 1990). This points to their possible involvement in transduction pathways of plant hormones such as abscisic acid.

The auxin regulation of anion channels first discovered in guard cells was recently described in cultured tobacco cells as well (Marten et al., 1991; Zimmermann et al., 1994). This points to a more general role for anion channels in auxin transduction cascades. Results obtained in parsley and soybean cell suspensions have revealed another possible role in signaling processes. These cells react to *Phytophtora megasperma*–derived elicitor preparations with a set of responses, including modifications in ion fluxes at the plasma membrane (K^+, H^+, Ca^{2+}, Cl^-), protein phosphorylation, and specific gene activation (reviewed in Ebel and Cosio, 1994). The fact that the whole set of these defense responses could be blocked by anion channel inhibitors raises the possibility of a dominating role of anion channels in a network that links the different ion channels and controls the specific terminal defense reaction.

The presence of anion channels seems to be ubiquitous in various tissues of algae and higher plants (reviewed in Tyerman, 1992). However, little is known concerning the physiology of anion channels in higher plant cells distinct from guard cells. Outwardly rectifying as well as inwardly rectifying conductances selective for chloride have been described on protoplasts from various species (Terry et al., 1991; Cerana and Colombo, 1992;

[1] To whom correspondence should be addressed.
[2] Current address: Max-Planck-Institut für Molekulare Pflanzenphysiologie, Karl-Liebknecht-Strasse 25, Haus 20, 14476 Golm, Germany.

Skerrett and Tyerman, 1994). Single anion channels have been described in protoplasts isolated from cultured cells (Schauf and Wilson, 1987; Lew, 1991). More recently, we have characterized voltage-dependent anion currents regulated by auxin and ATP in tobacco suspension-cultured cells (Zimmermann et al., 1994). In most cases, the studies concerned dedifferentiated cells that had most likely lost their original specificity, and information concerning channel regulation and function was lacking. To clarify the role of anion channels in whole plants, studying the organ- and tissue-specific activity of this channel type is necessary.

We investigated anion channels in protoplasts isolated from Arabidopsis plantlets to determine the organs in which the anion channels are present and how they are regulated in the plant. Because Arabidopsis is the object of many genetic and molecular biology studies (Meyerowitz, 1989), it represents one of the best models for detailed physiological studies in various genetic backgrounds. Nevertheless, relatively few studies have dealt with the regulation of its transmembrane ion exchanges (Lew, 1991; Spalding et al., 1991; Spalding and Goldsmith, 1993). We describe here an anion channel in epidermal cells of Arabidopsis hypocotyls, providing a new example of voltage-dependent anion channels in a specific cell type distinct from the guard cell. We show that Arabidopsis hypocotyl anion channels are able to switch between two modes characterized by different voltage dependences and different kinetic behaviors. This switch between a fast and a slow mode is controlled by ATP, as has been observed for anion channels in tobacco suspension cells (Zimmermann et al., 1994). In addition to the modulation of the whole-cell currents, we describe ATP-dependent regulation of the single-channel activity in excised patches from Arabidopsis hypocotyl protoplasts.

RESULTS

A Voltage-Dependent Anion Current Is Activated by Depolarization

Whole-cell currents of hypocotyl epidermal protoplasts from Arabidopsis plantlets were studied using the patch–clamp technique. When an intracellular solution containing 5 mM ATP was used, a voltage-dependent inward current increased during the first minutes after establishment of the whole-cell configuration. Figure 1A illustrates that depolarizing steps from −154 to −134, −124, and −114 mV induced inward currents with time constants in the millisecond range. The time course of activation was voltage dependent, the activation becoming faster for more depolarized potentials. The steady state I-to-V curve derived from voltage pulses between −154 and +36 mV shows that this current reached a maximal amplitude for membrane potentials at approximately −100 mV (E_{peak} of −101 ± 6 mV, where E stands for membrane potential, and n = 20, where n stands for the number of protoplasts tested; Figure 1B).

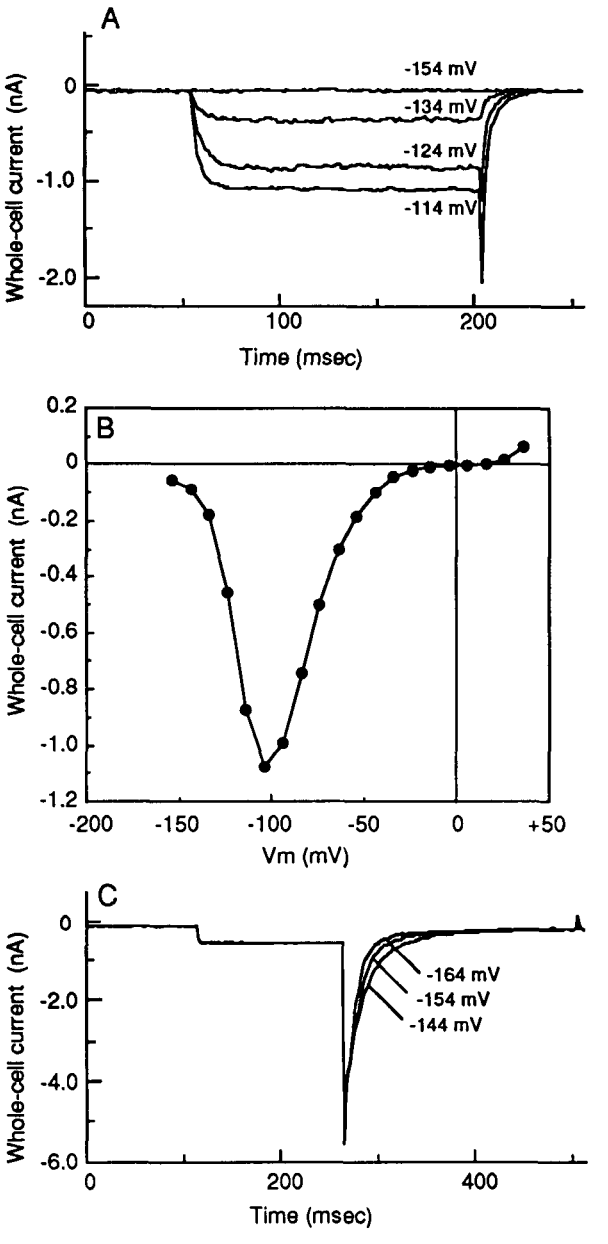

Figure 1. Voltage-Dependent Anion Currents at the Plasma Membrane of Arabidopsis Hypocotyl Protoplasts.

The experiments were performed 6 to 8 min after the whole-cell configuration was established using a pipette solution complemented with 5 mM Mg-ATP and a 50-mM $CaCl_2$ external bath. The protoplast was maintained at a V_{hold} (holding potential) of −154 mV.

(A) Activation kinetics of the anion current upon 150-msec depolarizing pulses to −134, −124, and −114 mV.

(B) I-to-V curve of the steady state anion currents measured 140 msec after the onset of voltage pulses to membrane potentials between −154 and +36 mV in 10-mV increments.

(C) Deactivation kinetics of the anion current. After a depolarizing pulse to −84 mV, V_m (applied membrane potential) was stepped back to −164, −154, and −144 mV.

The amplitude of the steady state current decreased for potentials more negative than −100 mV (Figure 1B), and the current was completely deactivated for potentials negative to −130 mV. Stepping back from −84 mV toward membrane potentials more hyperpolarized than −120 mV allowed study of the current deactivation (Figure 1C). The deactivation occurred with time constants in the millisecond range. The time course for deactivation was also voltage dependent, with time constants decreasing for hyperpolarized potentials (Figure 1C and Table 1).

For potentials more positive than −30 mV, the conductance was reduced and reversion was observed leading to outward currents. The reversal potential, +9 ± 8 mV (n = 7), measured in 50 mM external $CaCl_2$, was close to the Nernst equilibrium potentials for chloride and magnesium (E_{Cl} and E_{Mg} were +9 and +12 mV, respectively) and quite far from the equilibrium potential for any other ion (E_K was more negative than −150 mV; E_{Ca} and E_H were +140 and +93 mV, respectively). When 90% of the internal chloride was replaced by the impermeant anion glutamate, the inward current was reduced to amplitudes <50 pA at the peak potential (n = 3, compared with ~1 nA in Figure 1B), in agreement with the change in the chloride gradient. The reversal potential of the current (E_{rev} of −32 ± 7 mV; n = 3) was shifted toward the new equilibrium potential for chloride (E_{Cl} of −44 mV), whereas E_{Mg} was unchanged. These experiments demonstrate that the observed current was carried mainly by chloride ions.

This anion current was found in 80% (n = 61) of the protoplasts studied. In the other protoplasts (20%), only an outward current (possibly a potassium current) that disappeared within 2 min could be observed. The voltage-dependent and kinetic features of the anion current were maintained throughout the whole-cell recording when an intracellular solution containing ATP was used. However, the amplitude of the inward currents changed during the experiment. In the first phase after the entry in the whole-cell configuration, the maximal amplitude of the current increased from low (<100 pA) or zero amplitudes to amplitudes in the nanoampere range. After 1 to 5 min of stability, the current amplitude started to decrease, and in most cases, the current disappeared completely within 15 to 30 min. Figure 2 displays an example of the evolution of the current amplitude during a whole-cell experiment.

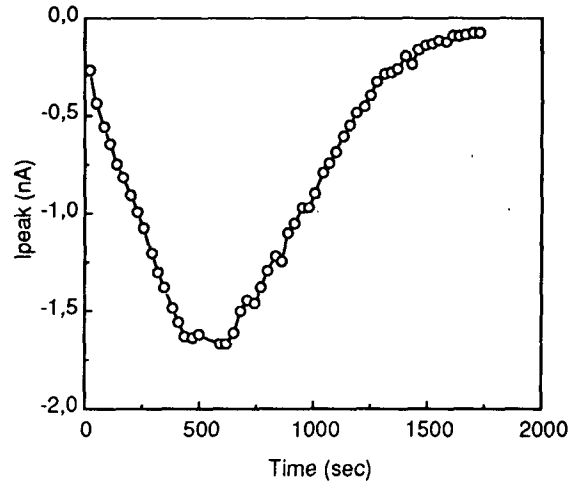

Figure 2. Time-Dependent Variations of the Amplitude of the Voltage-Dependent Anion Current.

A 3-sec voltage ramp between −154 and +36 mV was applied every 30 sec from a V_{hold} of −154 mV. The anion current amplitude at the peak (Ipeak) is displayed as a function of time after establishment of the whole-cell configuration.

The phytohormone auxin was shown to modify the gating of voltage-dependent anion channels in guard cells (Marten et al., 1991) and in tobacco cells (Zimmermann et al., 1994). To test auxin effects on Arabidopsis whole-cell anion currents, seals with high-access resistance (10 to 15 MΩ compensated at 85 to 90%) were selected to obtain stable anion currents with retarded rundown. Naphthaleneacetic acid (1-NAA), a synthetic active auxin, was applied at a concentration of 75 μM in various conditions: either in a 10 mM (n = 5) or in a 50 mM (n = 6) $CaCl_2$ external solution, either with buffered internal calcium (2 mM EGTA, 1 μM free calcium, n = 8) or with nearly unbuffered internal solution to allow intracellular free calcium changes (0.1 mM EGTA, no calcium added, n = 3). No effect could be seen in the 2 to 5 min after auxin application on Arabidopsis anion channel in any of the conditions tested, whereas this 1-NAA concentration induces, in the same time scale, a maximal response in both guard cells and tobacco cells. However, auxin effects that could occur on a time scale >5 min could not be monitored because of changes in both current amplitude and peak potential associated with the rundown.

Table 1. Deactivation of the Hypocotyl Anion Channel in the Fast and Slow Modes[a]

	+ATP		−ATP
V_m (mV)	τ Deactivation (msec) Activation at −84 mV	τ Deactivation (msec) V_{hold} = −4 mV	τ Deactivation (msec) V_{hold} = −4 mV
−144	4.2 ± 1.4 (n = 5)	4.6 ± 2.5 (n = 13)	2487 ± 1915 (n = 6)
−164	1.8 ± 0.5 (n = 5)	2.2 ± 1.4 (n = 13)	1059 ± 922 (n = 5)
−184	ND[b]	1.2 ± 0.7 (n = 12)	314 ± 124 (n = 4)

[a] In the whole-cell configuration, the membrane potential V_m was stepped back to the values indicated, either after an activating pulse from −154 to −84 mV or directly from a holding potential (V_{hold}) of −4 mV. Time constants (τ) for deactivation are given as mean value ± SD (n is the number of protoplasts tested). Deactivating currents were recorded using Clampex and fitted by exponential functions using Clampfit. +ATP, fast mode; −ATP, slow mode.

[b] ND, not determined.

In the Absence of Intracellular ATP, the Current Switches to a Slow Mode

When ATP was omitted in the intracellular solution, the inward current was again found in 80% of the protoplasts (n = 62), but changes affecting both its voltage regulation and its kinetics occurred. We applied sequences of the voltage protocol shown in Figure 3A to study the time-dependent behavior of the whole-cell current response (Figure 3B). After an increase in the current similar to the one described in the presence of ATP, the deactivation at −154 mV became slower and incomplete between 5 and 10 min after establishment of the whole-cell configuration, as shown in Figure 3. More generally, a loss of the fast deactivation for potentials negative to −140 mV was observed in 80% (n = 50) of the protoplasts displaying inward currents. The other 20% corresponded either to low-access conductance whole-cell seals or to rapid rundown occurring before any change in kinetics could be observed.

Figure 4 shows a comparison between voltage steps from a holding potential of −4 mV toward potentials between −184 and +36 mV recorded either in the presence of intracellular ATP or in the absence of ATP after the loss of the fast deactivation. After 5 to 15 min (depending on access conductance), the deactivation time course was much slower in the absence of ATP (τ between 725 and 5986 msec at −144 mV; Figure 4B and Table 1). Although a high variability of the time constants was observed, they were always at least two orders of magnitude higher than they were in the presence of ATP in

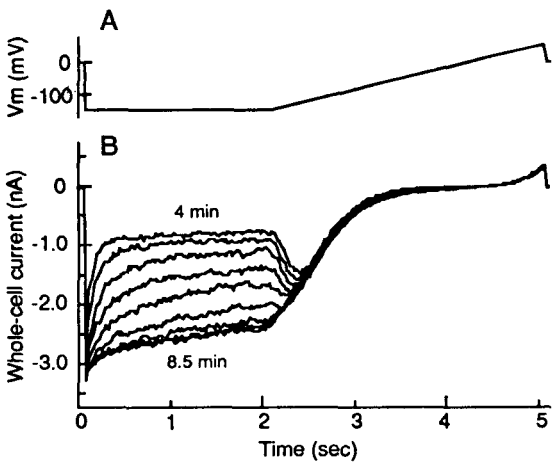

Figure 3. ATP-Dependent Regulation of the Anion Current.

(A) Voltage protocol. A 2-sec voltage step allowing the study of the deactivation kinetics at −154 mV was followed by a 3-sec voltage ramp from −154 to +36 mV, allowing the study of the voltage-dependent behavior of the current.

(B) Time-dependent change in the anion current upon intracellular perfusion using a pipette solution devoid of ATP. The protocol illustrated in **(A)** was repeated every 30 sec (V_{hold} of −4 mV) between 4 and 8.5 min after the whole-cell configuration was established.

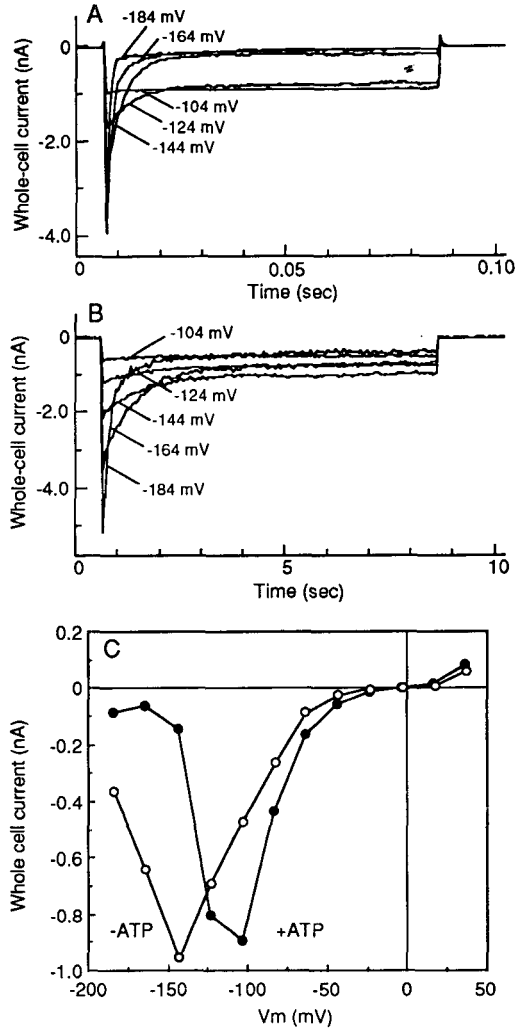

Figure 4. Features of the Slow and Fast Modes of the Anion Current.

(A) Deactivation kinetics of the Arabidopsis anion channel in the fast mode. The experiment was performed 6 min after the whole-cell configuration was established, using a pipette solution complemented with 5 mM ATP and a 50-mM $CaCl_2$ external solution. Currents were measured in response to 80-msec voltage pulses to potentials between −184 and −104 mV in 20-mV increments.

(B) Deactivation kinetics of the Arabidopsis anion channel in the slow mode. The experiment was performed 10 min after the establishment of the whole-cell configuration using a pipette solution devoid of ATP and a 50-mM $CaCl_2$ external solution. Currents were measured in response to 8-sec voltage pulses to potentials between −184 and −104 mV in 20-mV increments. Note the 100-fold contracted time scale compared with that in **(A)**.

(C) Comparison of the steady state I-to-V curves in the fast (+ ATP, closed circles) and slow (− ATP, open circles) modes. The I-to-V curves were derived from measurements of the currents, 70 msec or 7 sec after the onset of voltage pulses between −184 and +36 mV, with 20-mV increments in the fast (see **[A]**) and slow (see **[B]**) modes, respectively.

the pipette (τ between 0.5 and 10.2 msec at −144 mV; Figure 4A and Table 1). The current still displayed a voltage-dependent behavior (Figure 4C), but deactivation was largely incomplete. Only 67 ± 18% (n = 7) and 44 ± 24% (n = 7) of the current deactivated at −164 and −144 mV, respectively. In contrast, when the internal concentration of ATP was reduced to 0.1 mM, rapid deactivation was maintained (mean value of 14.9 ± 7.6 msec, n = 4, at −144 mV).

Without ATP, the reversal potential was +9 ± 5 mV (n = 23), indicating that the selectivity of the current was unchanged after the switch between fast and slow modes. The current underwent rundown with the same time course as it did in the presence of ATP, that is, usually after the switch between fast and slow modes. Thus, ATP regulates the channel by drastically changing the channel kinetics as well as by modifying the range of potentials for which the channel is active, but it neither alters its selectivity nor changes its rundown behavior.

Single Anion Channels Identified in the Outside-Out Configuration Are Conducting the Voltage-Dependent Whole-Cell Anion Current

To correlate the whole-cell current with single-channel characteristics, we studied single anion channel activity in outside-out patches. The excision from whole-cell seals was performed after the current had activated (within 5 min). The single-channel recordings were analyzed for current amplitudes and open and closed times at membrane potentials of −30, −60, −90, and −120 mV.

Single-channel activities were recorded in the presence of intracellular ATP with three different bath solutions containing 10 (n = 3), 50 (n = 5), and 100 mM (n = 3) $CaCl_2$. The single-channel I-to-V curves shown in Figure 5 were linear between −120 and −30 mV, allowing the determination of reversal potential and of single-channel conductance. The extrapolated reversal potentials were +47, +13, and −4 mV in 10, 50, and 100 mM $CaCl_2$ extracellular solutions, respectively. These reversal potentials were, in all three situations, close to the theoretical equilibrium potentials for chloride (E_{Cl} was +42, +9, and −8 mV in 10, 50, and 100 mM $CaCl_2$, respectively), demonstrating that the single channels recorded corresponded to anion channels. The single-channel conductances were 11, 21, and 20 pS in 10, 50, and 100 mM $CaCl_2$ external solutions, respectively. The single-channel conductance increased when the $CaCl_2$ concentration was raised from 10 to 50 mM, whereas the transmembrane chloride gradient was reduced. This indicates that either external chloride or external calcium regulates permeation through the anion channel pore, as proposed by Hedrich et al. (1994). The modulation of the single-channel conductance is saturated for 50 and 100 mM $CaCl_2$.

Between −60 and −120 mV, the single-channel open probabilities decreased from 0.720 ± 0.013 (n = 3) to 0.024 ± 0.012 (n = 4) in 50 mM $CaCl_2$ (Figure 6A) and from 0.162 ± 0.047 (n = 3) to 0.021 ± 0.017 (n = 3) in 10 mM $CaCl_2$, in accordance with the voltage-dependent decrease of the whole-cell current for potentials more hyperpolarized than −100 mV in the presence of ATP (Figure 1B). The channels observed in the outside-out configuration underwent rundown, as did anion currents in the whole-cell configuration. The rundown occurred by reduction of the number of active channels. It was thus possible to study the single-channel activity when only one channel was still fully active in the patch, allowing a precise determination of single-channel open probability.

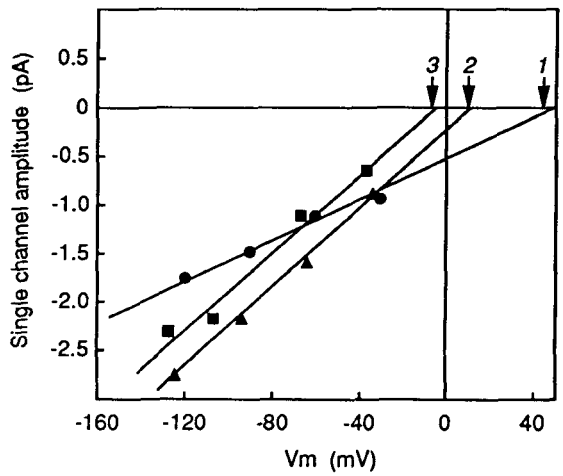

Figure 5. Chloride Selectivity of Single Channels Recorded in the Outside-Out Configuration.

Single-channel I-to-V curves in 10-mM (1, circles), 50-mM (2, triangles), and 100-mM (3, squares) $CaCl_2$ external solutions are shown. The pipette solution contained 5 mM Mg-ATP. Each curve was constructed from at least three independent experiments. In each experiment, amplitude histograms for various potentials were constructed and fitted by a Gaussian function. The arrows indicate the equilibrium potential for chloride in 10 mM (1, +42 mV), 50 mM (2, +9 mV), and 100 mM (3, −8 mV) $CaCl_2$.

The Channels Involved in Rapid and Slow Modes Have the Same Conductance, but Their Open Probabilities Are Differently Regulated by Voltage

Figure 6 shows a comparison of single-channel activities in outside-out patches made using a pipette solution either containing 5 mM ATP as given above (Figure 6A) or without ATP (Figure 6B); in the latter case, the patch was excised after the switch to the slow mode. Both pipette solutions were tested using a 50 mM $CaCl_2$ extracellular solution. The I-to-V relationships determined in these two conditions (Figure 6C) show that neither the single-channel conductances nor the reversal potentials were significantly different, supporting the idea that the same channel is responsible for the fast and slow modes observed in the whole-cell configuration.

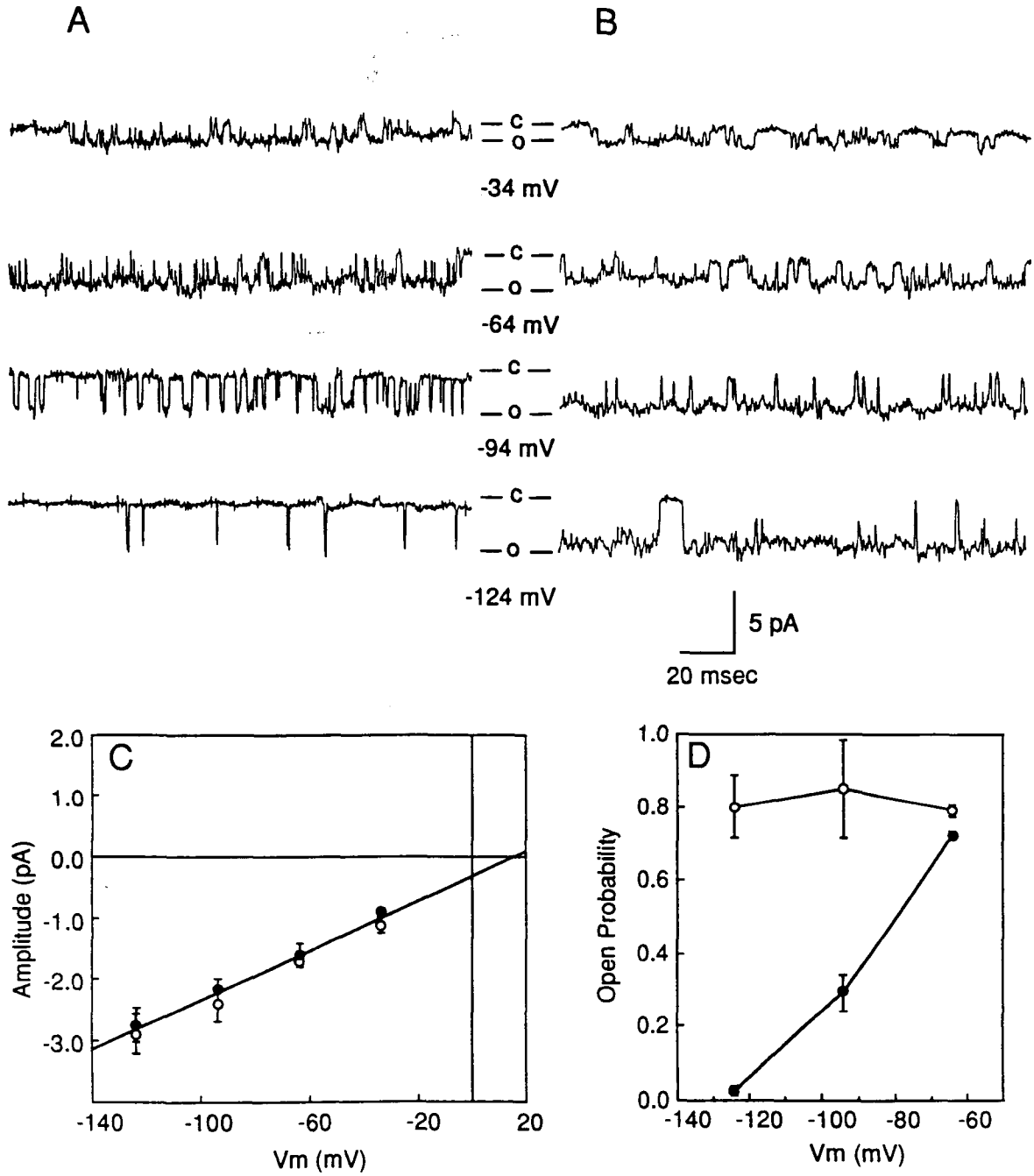

Figure 6. Slow and Fast Modes of the Arabidopsis Anion Channel in the Outside-Out Configuration.

(A) and **(B)** Channel currents were recorded from outside-out patches clamped at −34, −64, −94, and −124 mV. In the fast mode shown in **(A)**, the outside-out patch was excised 8 min after the whole-cell configuration was established, perfusing the intracellular medium with a pipette solution complemented with 5 mM Mg-ATP. In the slow mode shown in **(B)**, the outside-out patch was excised 12 min after the whole-cell configuration was established, that is, after the switch from fast to slow mode, using a pipette solution devoid of ATP. c, closed state; o, open state.

(C) Single-channel I-to-V curves in the slow (open circles) and fast (closed circles) modes in a 50-mM $CaCl_2$ external solution. Recordings were analyzed as given in Figure 4.

(D) Open probability of single anion channels in the fast (closed circles) and slow (open circles) modes. The open probability was calculated as open time per total time during a 30-sec recording displaying only one active channel, that is, one open level at −64 mV.

(C) and **(D)** show mean values ± SD from three to five outside-out patches.

In contrast, Figure 6D shows that the voltage regulation of single-channel open probabilities diverged between the fast and slow modes. Whereas, in the presence of cytosolic ATP, the open probabilities decreased drastically between −64 and −124 mV, in the absence of cytosolic ATP, the open probabilities were maintained at 0.790 ± 0.020 (n = 3) and 0.800 ± 0.100 (n = 4) for −64 and −124 mV, respectively. This finding agreed with the voltage regulation observed in the whole-cell configuration: the rapid current (with internal ATP) decreased for potentials negative to −100 mV, whereas voltage-dependent deactivation occurred only for potentials more negative than −150 mV for the slow current (without ATP; see Figure 4C).

Studying the distribution of open and closed time allowed us to determine the kinetic features of the open and closed states of the channel (Table 2). In the presence of intracellular ATP, (1) a decrease in the mean lifetime of the open state from 6.9 ± 2.5 msec (n = 3) to 0.6 ± 0.2 msec (n = 4), and (2) the appearance of a novel closed state at −124 mV characterized by a long lifetime (49.9 ± 7.6 msec, n = 4) underlie the strong decrease of the single-channel open probability between −64 and −124 mV. In the absence of intracellular ATP, the single-channel behavior at −64 mV was comparable with the situation, including ATP, but at −124 mV, neither the lifetime of the open state nor the mean lifetime of the closed state changed significantly (Table 2), and no additional closed state appeared. These results show that a complex switch in the gating mode of the channel occurs between the fast and slow modes.

DISCUSSION

The discovery of voltage-dependent anion channels in protoplasts isolated from Arabidopsis hypocotyl epidermal cells provides additional evidence that this channel type is more widespread than was formerly thought. Initially, such channels were described only in guard cell protoplasts (Keller et al., 1989) and more recently in tobacco cell suspensions (Zimmermann et al., 1994). From our work on hypocotyl protoplasts, we now raise the issue of the tissue-specific expression pattern of voltage-dependent anion channels. We observed the anion current not only in 80% of the hypocotyl epidermal protoplasts but also in some protoplasts from parenchyma cells (S. Thomine, unpublished results). Other organs must be investigated to obtain a more general view of the expression pattern of this channel, which may give a first hint to its functional role in the plant.

We argue that in Arabidopsis a single type of anion channel can switch between two modes with distinct functional properties. Transition between rapid and slow anion currents has also been observed in guard cells (Schroeder and Keller, 1992; Dietrich and Hedrich, 1994) and in cultured tobacco cells (Zimmermann et al., 1994). In Arabidopsis, the transition between fast and slow modes is controlled by intracellular ATP. This type of regulation is similar to what we have already described for the anion conductance of protoplasts isolated from tobacco cell suspensions (Zimmermann et al., 1994). Conservation of such an ATP-dependent regulation between two different species and in different cell types supports the idea that it may play an important role in the plant cell physiology.

The effect of ATP depletion can reflect either a metabolic regulation of the channel or a requirement of this molecule as a substrate for phosphorylations. We have investigated the chloride current using a low internal ATP concentration of 0.1 mM, a concentration shown to occur in plant cells under stress conditions when their energy charge is reduced (Saint-Ges et al., 1991; Gout et al., 1992). If the ATP modulation of the channel reflects a metabolic regulation, low values of ATP concentrations in the physiological range should induce a switch to the slow state. In contrast, the current still displayed fast kinetics with 0.1 mM intracellular ATP. Thus, the nucleotide dependence probably corresponds instead to the involvement of phosphorylation/dephosphorylation processes, as in the tobacco suspension cells (Zimmermann et al., 1994). An even more complex nucleotide regulation of ion channel activity also would be possible, as shown in animal cells. A prominent example of two-stage modulation is the chloride conductance connected with cystic fibrosis (CFTR), possessing both protein kinase A phosphorylation sites and nucleotide binding sites (Welsh et al., 1992). In the present study using Arabidopsis hypocotyl protoplasts, the regulation of the voltage-dependent whole-cell current by ATP could be correlated with gating mechanisms at the single-channel level. The presence of ATP

Table 2. Mean Lifetime of Open and Closed States in the Fast and Slow Modes of the Hypocotyl Anion Channel[a]

	+ATP				−ATP		
V_m (mV)	n	Closed State τ1 ± SD (msec)	Closed State τ2 ± SD (msec)	Open State τ1 ± SD (msec)	n	Closed State τ1 ± SD (msec)	Open State τ1 ± SD (msec)
−64	3	0.8 ± 0.1	–	6.9 ± 2.5	3	0.8 ± 0.3	6.2 ± 2.2
−94	5	4.0 ± 0.8	–	1.9 ± 0.6	3	1.1 ± 0.8	9.5 ± 2.6
−124	4	2.2 ± 0.3	49.9 ± 7.6	0.6 ± 0.2	4	0.5 ± 0.3	12.1 ± 4.7

[a] Histograms of the open and closed time distributions derived from the analysis of n outside-out recordings displaying only one open level were fitted by exponential functions using the pSTAT program. Notations are as given for Table 1. τ1 and τ2 stand for mean lifetimes characterizing short- and long-lived states of the channel, respectively. Dashes indicates that only one state could be detected.

modulates the mean lifetimes of the open and closed states of the channel at hyperpolarized potentials, thus controlling its open probability.

Our data also indicate that the hypocotyl anion channel is regulated by other mechanisms. This channel undergoes rundown in both fast and slow modes in the whole-cell configuration as well as in excised membrane patches. This indicates that the cytoplasm's loss of integrity due to entry in the whole-cell configuration disrupts a mechanism necessary to maintain the channel in an activated state. To prevent the rundown, several attempts have been made to complement the pipette solution: adding, for example, protease inhibitors to block a rapid turnover of the channel protein, DTT to maintain the cytosol in a reduced redox state during the experiment, and GTP to interfere with G-protein regulatory mechanisms. None of these treatments has been efficient in preventing the rundown, and the intracellular component or the mechanism required to maintain channel activity has not been identified.

A possible effect of auxins on the anion channel was examined in Arabidopsis hypocotyl cells. Such a modulation has been conserved between guard cells and tobacco suspension-cultured cells (Marten et al., 1991; Zimmermann et al., 1994) but could not be shown on the Arabidopsis anion channel in the time scale that allows maximal response in both other systems. This result suggests that this channel is not directly regulated by auxin, in contrast with the hypothesis raised for the guard cell anion channel (Marten et al., 1991). Further investigations are needed to explore an indirect modulation of the channel by auxin. The lack of effect observed here may originate either from the loss of factors coupling auxin perception to channel modulation during the perfusion of the cytoplasm or from the fact that the channel was studied on hypocotyls at the end of the elongation phase in which auxin perception may be down-regulated.

Two main physiological roles can be proposed for the hypocotyl anion channels in connection with the existence of fast and slow modes. In the mode displaying fast deactivation maintained only in the presence of intracellular ATP, the channels are closed at resting potentials measured in hypocotyl cells (approximately −180 mV in *Nicotiana plumbaginifolia* seedlings; Stirnberg et al., 1995). Anion efflux can occur only if the channels are activated by a previous depolarization and the activation itself contributes to further membrane depolarization. This amplification may be involved either in the transduction of external signals into cells or in the transmission of action potential–like signals between cells (Wildon et al., 1992). Alternatively, a signal may activate the channel without previous depolarization if it shifts the activation potential of the channel toward the resting potential as recently shown, for example, for malate (Hedrich and Marten, 1993).

The channel is found initially in the fast mode before the cytoplasm is perfused with an internal solution depleted of ATP (see Figure 3), indicating that it corresponds to the resting state of the channel. Switching toward the slow mode represents an alternative gating mode for the anion conductance. In this state, the conductance deactivates only partially at resting potentials. Thus, anion channels open and enable a sustained efflux of anions from the cell with no requirement for any previous depolarization. Their opening, together with an outward-rectifying potassium channel, would lead to salt efflux and thus to decrease in cell turgor. Such a role in osmoregulation has been demonstrated for the slow anion channel in guard cells (Schroeder et al., 1993). A similar role can be postulated in hypocotyl epidermal cells, where activation of the anion channel would result in the inhibition of elongation.

The study of Arabidopsis mutants impaired in their response to various signals, such as plant hormones (Giraudat et al., 1994; Hobbie et al., 1994) or light (Deng, 1994), as well as in osmotic regulation, will help to clarify the physiological role of the hypocotyl anion channel.

METHODS

Plant Material

Plantlets (*Arabidopsis thaliana* ecotype Columbia) were grown on a medium containing 5 mM KNO_3, 2.5 mM K_2HPO_4/KH_2PO_4, pH 6, 2 mM $MgSO_4$, 1 mM $Ca(NO_3)_2$, 1 mM Mes, 50 μM FeEDTA, Murashige and Skoog (1962) microelements, 10 g/L sucrose, and 7 g/L agar. Culture conditions were 21°C, with a 16-hr daylength at lighting levels of 120 μE m^{-2} sec^{-1}, using neon tubes (in combination from Mazdafluor Blanc Industrie and Mazdafluor Prestiflux, Mazda Eclairage, France). Plantlets 8 to 14 days old were used for electrophysiological investigations. This stage corresponds to the end of hypocotyl elongation and the emergence of the first leaves.

Protoplast Isolation

Hypocotyls were excised from 30 to 40 plantlets, and protoplasts were isolated according to Elzenga et al. (1991). After excision, the hypocotyl segments were transferred in a hyperosmotic solution (solution A: 2 mM $CaCl_2$, 2 mM $MgCl_2$, 0.1% Gamborg's B5 vitamins, 10 mM Mes/KOH, pH 5.5, osmolality adjusted to 600 mOsmol with mannitol, using a vapor pressure osmometer [model 5500; Wescor, Logan, UT]) to plasmolyze the cells. The hypocotyls were incubated for 15 min at 26°C under gentle agitation (70 rpm) in solution A complemented with cell wall–degrading enzymes (1.7% cellulase RS [Yakult Honsha, Tokyo, Japan], 1.7% cellulysin [Calbiochem], 0.026% pectolyase Y23 [Seishin, Tokyo, Japan], and 0.2% BSA [Sigma]). The hypocotyls with partially degraded cell walls were then washed, that is, the incubation medium was removed and the hypocotyls were resuspended twice in solution A during 5 min under gentle agitation (70 rpm). Virtually no protoplast was released during these steps. Solution A was subsequently replaced by a hypo-osmotic solution (solution B: 2 mM $CaCl_2$, 2 mM $MgCl_2$, 10 mM K-citrate, 2 mM Mes-Tris, pH 5.5, osmolality adjusted to 280 mOsmol with mannitol, using a vapor pressure osmometer as above). This procedure induced the swelling and release of the protoplasts. This step was monitored visually under the microscope, allowing us to determine the origin of the protoplasts. The protoplasts came out through the section of the hypocotyls. Three main classes

of protoplasts were distinguished: (1) small protoplasts with diameters of <15 μm and heterogenous aspects that originated from the different cell types of the stele; (2) large protoplasts with a mean diameter of 60 μm (diameters between 30 and 90 μm) and abundant chloroplasts that originated from the cortical parenchyma; and (3) protoplasts with a mean diameter of 40 μm (diameters between 25 and 75 μm) that originated from epidermal cells. Protoplasts with moderate size and active cyclosis that belonged to this last class were used for patch-clamp experiments. Protoplast release was continued in solution B for 15 to 20 min. Then the protoplasts were separated from the hypocotyls by filtration (pore diameter, 300 μm) and dispatched in the patch-clamp chambers. They were allowed to settle on the glass bottom for 30 to 60 min before perfusion with the external patch-clamp solution (see composition below).

Electrophysiological Investigations

Patch-clamp experiments were performed as described by Hamill et al. (1981) using an amplifier (model 200A; Axon Instruments, Foster City, CA). During measurements, freshly isolated epidermal protoplasts from Arabidopsis hypocotyls were maintained in bathing medium (10, 50, or 100 mM $CaCl_2$, 5 mM $MgCl_2$, 10 mM Mes-Tris, pH 5.6). The pipettes were filled with 150 mM KCl, 2 mM $MgCl_2$, 2 mM EGTA, 1.8 mM $CaCl_2$, 10 mM Tris-Mes, pH 7.2, supplemented with 5 mM Mg-ATP. The osmolalities of both solutions were adjusted to 450 mOsmol with mannitol, using a vapor pressure osmometer as above. Gigaohm resistance seals (1 to 10 GΩ) between pipettes (pipette resistance, 1 to 5 MΩ) coated with Sylgard (General Electric, New York, NY) pulled from Kimax-51 capillaries (Kimble Glass, Inc., Owens, IL) and protoplast membranes were obtained with gentle suction, leading to whole-cell configuration. The liquid junction potentials were measured according to Neher (1992). With the 50 mM $CaCl_2$ bath solution, the junction potentials were +4 mV when the standard pipette solution was used and +15 mV when 90% of the chloride was replaced by glutamate. The junction potentials were +7 mV and lower than +1 mV in 100 and 10 mM $CaCl_2$, respectively.

For whole-cell experiments, application of voltage programs and handling of the data were performed using a Digidata 1200 interface and patch-clamp software pClamp 5.5.1. with Clampex and Clampfit (Axon Instruments). The filter frequency was set to 2 kHz; the acquisition rate of data points in the whole-cell configuration depended on the voltage protocols and determined the time resolution of the current response. Capacitance and pipette offset potentials were compensated during the patch-clamp experiments. Only seals with low access resistance (<12 MΩ) were used for experiments, and the series resistance was compensated to >90% when necessary. No leak substraction was applied on any of the recordings.

Outside-out patches were obtained by withdrawing the pipette from the whole-cell configuration. The single-channel recordings were stored on videotape. For analysis, they were digitized with a sample rate of 0.1 msec (five times the filter frequency) using Fetchex (pClamp 5.5.1; Axon Instruments). Amplitudes and open and closed time lists were then generated using Fetchan in the event list mode (pClamp 5.5.1; Axon Instruments). Finally, the distribution of amplitudes was fitted by a Gaussian model in pSTAT (pClamp 5.5.1; Axon Instruments), and the distributions of open and closed times were fitted by exponential models.

Unless otherwise indicated, figures are shown for one representative protoplast, and statistics are given as mean ± SD (*n* indicates the number of protoplasts tested).

ACKNOWLEDGMENTS

This work was funded in part by the European Community's BIOTECH program, as part of the Project of Technological Priority 1993–1996. The authors thank Françoise Lelièvre and Juliette Barré for helping with Arabidopsis cultures and protoplast preparations as well as Geneviève Belliard and Geneviève Ephritikhine for providing Arabidopsis seeds.

Received July 3, 1995; accepted October 13, 1995.

REFERENCES

Cerana, R., and Colombo, R. (1992). K^+ and Cl^- conductance of *Arabidopsis thaliana* plasma membrane at depolarized voltages. Bot. Acta **105,** 273–277.

Deng, X.W. (1994). Fresh view of light signal transduction in plants. Cell **76,** 423–426.

Dietrich, P., and Hedrich, R. (1994). Interconversion of fast and slow gating modes of GCAC1, a guard cell anion channel. Planta **195,** 301–304.

Ebel, J., and Cosio, E.G. (1994). Elicitors of plant defense responses. Int. Rev. Cytol. **148,** 1–36.

Elzenga, J.T.M. (1991). Patch clamping protoplasts from vascular plants. Plant Physiol. **97,** 1573–1575.

Giraudat, J., Parcy, F., Bertauche, N., Gosti, F., Leung, J., Morris, P.-C., Bouvier-Durand, M., and Vartanian, N. (1994). Current advances in abscisic acid action and signalling. Plant Mol. Biol. **26,** 1557–1577.

Gout, E., Bligny, R., and Douce, R. (1992). Regulation of intracellular pH values in higher plant cells. Carbon-13 and phosphorus-31 nuclear magnetic resonance studies. J. Biol. Chem. **267,** 13903–13909.

Hamill, O.P., Marty, A., Neher, E., Sakmann, B., and Sigworth, F.J. (1981). Improved patch-clamp techniques for high-resolution current recording from cells and cell-free membrane patches. Pflügers Arch. **391,** 228–232.

Hedrich, R., and Marten, I. (1993). Malate-induced feedback regulation of plasma membrane anion channels could provide a CO_2 sensor to guard cells. EMBO J. **12,** 897–901.

Hedrich, R., Busch, H., and Raschke, K. (1990). Ca^{2+} and nucleotide-dependent regulation of voltage-dependent anion channels in the plasma membrane of guard cells. EMBO J. **9,** 3889–3892.

Hedrich, R., Marten, I., Lohse, G., Dietrich, P., Winter, H., Lohaus, G., and Heldt, H.-W. (1994). Malate-sensitive anion channels enable guard cells to sense changes in the ambient CO_2 concentration. Plant J. **6,** 741–748.

Hobbie, L., Timpte, M., and Estelle, M. (1994). Molecular genetics of auxin and cytokinin. Plant Mol. Biol. **26,** 1499–1520.

Keller, B.U., Hedrich, R., and Raschke, K. (1989). Voltage-dependent anion channels in the plasma membrane of guard cells. Nature **341,** 450–453.

Lew, R. (1991). Substrate regulation of single potassium and chloride ion channels in *Arabidopsis* plasma membrane. Plant Physiol. **95,** 642–647.

Marten, I., Lohse, G., and Hedrich, R. (1991). Plant growth hormones control voltage-dependent activity of anion channels in plasma membrane of guard cells. Nature **353,** 758–762.

Meyerowitz, E.M. (1989). Arabidopsis, a useful weed. Cell **56,** 263–269.

Murashige, T., and Skoog, F. (1962). A revised medium for rapid growth and bioassays with tobacco tissue cultures. Physiol. Plant. **15,** 473–497.

Neher, E. (1992). Correction for liquid junction potentials in patch–clamp experiments. Methods Enzymol. **207,** 123–131.

Saint-Ges, V., Roby, C., Bligny, R., Pradet, A., and Douce, R. (1991). Kinetic studies of the variations of cytoplasmic pH, nucleotide triphosphates (^{31}P-NMR) and lactate during normoxic and anoxic transitions in maize root tips. Eur. J. Biochem. **200,** 477–482.

Schauf, C.L., and Wilson, K.J. (1987). Properties of single K^+ and Cl^- channels in *Asclepias tuberosa* protoplasts. Plant Physiol. **85,** 413–418.

Schroeder, J.I., and Hagiwara, S. (1989). Cytosolic calcium regulates ion channels in the plasma membrane of *Vicia faba* guard cells. Nature **338,** 427–430.

Schroeder, J.I., and Hedrich, R. (1989). Involvement of ion channels and active transport in osmoregulation and signaling of higher plant cells. Trends Biol. Sci. **14,** 187–192.

Schroeder, J.I., and Keller, B. (1992). Two types of anion channel currents in guard cells with distinct voltage regulation. Proc. Natl. Acad. Sci. USA **89,** 5025–5029.

Schroeder, J.I., Schmidt, C., and Sheaffer, J. (1993). Identification of high-affinity slow anion channel blockers and evidence for stomatal regulation by slow anion channels in guard cells. Plant Cell **5,** 1831–1841.

Skerrett, M., and Tyerman, S.D. (1994). A channel that allows inwardly directed fluxes of anions in protoplasts derived from wheat roots. Planta **192,** 477–484.

Spalding, E.P., and Goldsmith, M.H.M. (1993). Activation of K^+ channels in the plasma membrane of Arabidopsis by ATP produced photosynthetically. Plant Cell **5,** 477–484.

Spalding, E.P., Slayman, C.L., Goldsmith, M.H., Gradmann, D., and Bertl, A. (1991). Ion channels in *Arabidopsis* plasma membrane. Plant Physiol. **99,** 96–102.

Stirnberg, P., King, P.J., and Barbier-Brygoo, H. (1995). An auxin-resistant mutant of *Nicotiana plumbaginifolia* Viv. is impaired in 1-naphthaleneacetic acid–induced hyperpolarization of hypocotyl cell membranes in intact seedlings. Planta **196,** 706–711.

Terry, B.R., Tyerman, S.D., and Findlay, G.P. (1991). Ion channels in the plasma membrane of Amaranthus protoplasts: One cation and one anion channel dominate the conductance. J. Membr. Biol. **121,** 223–236.

Tyerman, S.D. (1992). Anion channels in plants. Annu. Rev. Plant Physiol. Plant Mol. Biol. **43,** 351–373.

Welsh, M.J., Anderson, M.P., Rich, D.P., Berger, H.A., and Denning, G.M. (1992). Cystic fibrosis transmembrane conductance regulator: A chloride channel with novel regulation. Neuron **8,** 821–829.

Wildon, D.C., Thain, J.F., Minchin, P.E.H., Gubb, I.R., Reilly, A.J., Skipper, Y.D., Doherty, H.M., O'Donnell, P.J., and Bowles, D.J. (1992). Electrical signaling and systemic proteinase inhibitor induction in the wounded plant. Nature **306,** 62–65.

Zimmermann, S., Thomine, S., Guern, J., and Barbier-Brygoo, H. (1994). An anion current at the plasma membrane of tobacco protoplasts shows ATP-dependent voltage regulation and is modulated by auxin. Plant J. **6,** 707–716.